2008 American Control Conference
Westin Seattle Hotel, Seattle, Washington, USA
June 11-13, 2008

Autonomous vehicle control for ascending/descending along a potential field with two applications

Dimitar Baronov and John Baillieul

Abstract— **In this paper, we present a reactive control law that can navigate a single, sensor-enabled vehicle to ascend or descend a scalar potential field. The design builds on our previous work on developing an isoline following control. The model framework enables us to establish performance bounds for the developed ascending/descending control that are related to the geometrical parameters of the field. The efficacy of our approach is demonstrated through two possible applications - source-centric mapping of a potential field and tracking of a single target, emitting a distance-related potential field.**

I. INTRODUCTION

In the last few years there has been increased interest in what the authors of this paper call automated potential field exploration. A few references worth noting are [1]-[8]. The main motivation of this type of exploration is the existence of certain phenomena that can be measured at discrete points but which are impossible to be instantaneously sensed in their entirety. Examples in environmental monitoring are quantities such as ocean temperature, CO_2 concentration and many others that can be measured only in a point-wise fashion, so as to provide an arbitrarily accurate representation of their distribution. Going down the scale, similar restriction can be observed in Scanning Probe Microscopy (SPM) where a single probe measures the specifics of a few micrometers sample, such as elevation, magnetism and etc., point-by-point. The challenge is to find means for efficiently acquiring information either by focusing on certain features of the field such as level sets [1], [6], [7] and extremums [9], or by reducing the error of the acquired potential field map [2]. In general, these techniques are also known as non-raster scans [10]. The aim of this paper is to contribute to this idea by proposing a new control capable of navigating a vehicle, such that it ascends/descends along a potential field. Although similar exploration strategies are employed by other authors [3], [9], our control overcomes the deficiencies of the previously known techniques by introducing a purely reactive control which makes use of a single sensor enabled vehicle.

A reactive control law was also used in a our previous work [1] to guide an autonomous exploration agent to map the isolines of an unknown potential field. The label *reactive control* stands for the concept of treating the agent as a dynamical system reacting directly to its immediate environment. For the purpose of the automated potential field exploration such strategies can have two possible goals: to follow an isoline [1], [6] and to ascend/descend along the potential [3]. In the current paper, we build upon the general model framework established in [1] to design and analyze the descending/ascending control law. Our view is that the currently proposed algorithm, together with the isoline following control law, form a full set of motion primitives which a higher level strategy can utilize for the continuous monitoring and exploration of potential fields.

There are two known setups, that can provide for the solution of this problem. The first one, we call Single Entity equipped with Multiple Sensors (SEMS) - a single entity, represented either by a single vehicle or by a rigid formation of vehicles [11], utilizes multi-sensor information to achieve the objectives of the control law [3], [6]. The existence of a sensor array enables the control to rely on a variety of explicitly estimated parameters, describing the local behavior of the potential field, such as the direction and the magnitude of the gradient at a point or the curvature of an isoline.

In the current paper, we employ Single Entity equipped with Single Sensor (SESS) - the control law can rely only on a single point measurement of the potential field. (See [1] and [9] for other examples of SESS potential field exploration.) The benefits of such an approach are that: first, it is a more parsimonious use of resources; and second, it can be applied in a much smaller scale in which multiple sensors cannot be utilized [12].

The limitation of this setup is that no gradient information can be available in real time, since to estimate the magnitude and the direction of the gradient requires the potential to be measured at at least four points. One way to handle this restriction is algorithmic. Reference [9] presents a solution for the extremum seeking problem in which the vehicle moves in a given direction until the potential is increasing along its trajectory (or respectively decreasing depending on whether the extremum is a minimum or a maximum) and when the potential starts decreasing, the vehicle orients to another direction. Although an algorithmic approach presents a viable solution for the descending/ascending problem, it comes with innate limitations. Foremost, algorithmic controls are difficult or often impossible to analyze. For the automated potential field exploration this fact manifests by the inability of an algorithmic control to address the question of whether there are curtain pathological representations of the potential field that render it unstable. To the contrary, a reactive control law can have analytically established performance bounds that, if related to the geometry of the potential field, can quantify the limiting cases for the control.

In this paper, we show two possible applications for the ascending/descending control law. The first one is to map

This work was supported by ODDR&E MURI01 Program Grant Number DAAD19-01-1-0465, by ODDR&E MURI07 Program Grant Number FA9550-07-1-0528, and by the National Science Foundation ITR Program Grant Number DMI-0330171, all to Boston University.

D. Baronov and J. Baillieul are with the Department of Aerospace and Mechanical Engineering, Boston University, Boston, MA, 02215. {baronov, johnb}@bu.edu

a neighborhood of an extremum, such that the position of the extremum is mapped with pre-specified precision. The second application is to localize and continuously track a moving source.

II. Model framework for the reactive control of a vehicle in a potential field

Let $S : \mathbb{R}^2 \rightarrow \mathbb{R}$ be an almost everywhere analytic scalar potential field. The task of designing a reactive control is equivalent with defining a map $\Psi : \mathbb{R}^{n+1} \rightarrow \mathbb{R}^2$:

$$\Psi\left(S, \frac{dS}{dt}, ..., \frac{d^n S}{dt^n}\right) = \mathbf{U}, \tag{1}$$

which transforms the potential measured at the position of the vehicle and the history captured by its higher order derivatives into a control action $\mathbf{U}$. Here, $S = S(\mathbf{r}(\mathbf{t}))$ is the potential along the trajectory of the vehicle at time t and the vector $\mathbf{r}(t) \in \mathbb{R}^2$ is relative to a fixed coordinate frame.

The derivatives cannot be directly evaluated and need to be estimated from the measurements of the potential. Taking into account that the measurements in general have added noise, the higher the order of a derivative, the larger the noise of its estimate. Therefore, we limit the control to the form:

$$\mathbf{U} = \Psi\left(S, \frac{dS}{dt}\right). \tag{2}$$

As established in [1], a convenient coordinate system to analyze a reactive control is a nonlinear coordinate system, which coordinate directions are aligned with and transverse to the level sets of the potential function $S(\mathbf{r})$. Assuming that S is a harmonic function implies that a coordinate system based on S and its harmonic conjugate Q, satisfying:

$$\frac{\partial Q}{\partial x} = -\frac{\partial S}{\partial y} \tag{3}$$

$$\frac{\partial Q}{\partial y} = \frac{\partial S}{\partial x}, \tag{4}$$

is orthogonal and defined everywhere in $\mathbb{R}^2$.

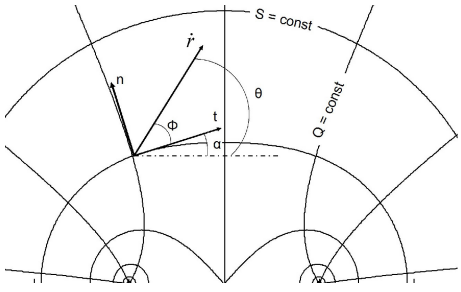

Fig. 1. Angles between the velocity of the vehicle and the normal $\vec{n} = \frac{\nabla S}{|\nabla S|}$ and the tangent $\vec{t} = \frac{\nabla Q}{|\nabla Q|}$ to the isoline, along which S has constant value.

The conventional wisdom of designing control for autonomous agents is that, regardless of the goal, the simplest model, e.g the fully actuated point vehicle, provides for a least complex solution. This model can be written as:

$$\dot{\mathbf{r}} = \mathbf{U}, \tag{5}$$

where the control should be $\mathbf{U} = \{u, v\}^T$ and consists of the projections of the velocity of the vehicle on the x and y axis of the fixed coordinate frame.

However, the specifics of the SESS setup leads to a situation for which the simplest model does not provide for the simplest solution. Previously this fact has been shown in [1] and it can be observed from the curvilinear representation of (5):

$$\dot{S} = \nabla S \cdot \dot{\mathbf{r}} = -VM \sin(\theta - \alpha) \tag{6}$$

$$\dot{Q} = \nabla Q \cdot \dot{\mathbf{r}} = VM \cos(\theta - \alpha). \tag{7}$$

In these equations the parameters are defined as follows: $V = \sqrt{u^2 + v^2}$ is the magnitude of the velocity, M is the magnitude of the gradient ($\|\nabla S\|$), α is the angle between the tangent of the isoline at the position of the robot and the x axes, and θ is the heading of the vehicle (Fig.1).

Since the goal of a reactive potential field control is to align the vehicle either to the level sets (isoline following $\sin(\theta - \alpha) = 0$) or to their transverse (gradient climbing $\cos(\theta - \alpha) = 0$), the vehicle should be able to estimate the angle α, or in other words the direction of the gradient. The SESS setup excludes such information. Nevertheless, introducing nonholonomic constraints on the vehicle, or $\mathbf{U} = \{V, \omega\}^T$ ($\omega = \dot{\theta}$), alleviates this limitation.

Using the simplest example of a nonholonomic vehicle:

$$\dot{\mathbf{r}} = V\begin{pmatrix} \cos\theta \\ \sin\theta \end{pmatrix} \tag{8}$$

$$\dot{\theta} = \omega, \tag{9}$$

defining $\phi = \theta - \alpha$, and setting constant unit velocity yields to the following system in the $\{S, Q\}$ plane:

$$\begin{aligned} \dot{S} &= -M \sin\phi \\ \dot{Q} &= M \cos\phi \\ \dot{\phi} &= \omega - \kappa_S \cos\phi - \kappa_Q \sin\phi. \end{aligned} \tag{10}$$

Here, $\nabla \cdot \left(\frac{\nabla S}{|\nabla S|}\right) = \kappa_S$ and $\nabla \cdot \left(\frac{\nabla Q}{|\nabla Q|}\right) = \kappa_Q$ are the curvatures respectively of the isolines $S(\mathbf{r}) = const$ and the streamlines $Q(\mathbf{r}) = const$. Note that in this expression all the unknown parameters (κ_S, κ_Q and M) are geometrical characteristics of the potential field. Using non-unit velocity will scale this parameters with the magnitude of the speed. However, in what follows we treat them as disturbances and therefore choosing constant speed allows us to define exact bounds on their influence. This fact enables the design of a control law which performance depends purely on the geometry of the potential field.

III. Ascending/descending control

In this section we introduce the ascending/descending control law. To facilitate the analysis, the discussion that follows is aimed at ascending control ($\dot{S}(\mathbf{r}(t)) > 0$). However, without loss of generality, the results can be extended to descending control ($\dot{S}(\mathbf{r}(t)) < 0$).

We start by defining bounds on the geometry of the potential field. Foremost, to enable the design of an ascending control law, the potential should be steep enough. This requirement is formalized in the following assumption:

Assumption 1: Let $\Omega_S = \left\{\mathbf{r} \in \mathbb{R}^2 | S(\mathbf{r}) \geq S_d\right\}$ be a given region on the plane in which the vehicle executes its motion, and let there be a single maximum in Ω_S with potential value S_{max}. Then, for every $0 < \epsilon < S_{max} - S_d$, which defines a neighborhood $\Omega_M = \left\{\mathbf{r} \in \mathbb{R}^2 | S(\mathbf{r}) \geq S_{max} - \epsilon\right\}$ around the maximum, there exists σ such that $\|\nabla S\| > \sigma$, $\forall \mathbf{r} \in \Omega_S - \Omega_M$.

The curvatures κ_S and κ_Q quantify the deformation of the potential field. It follows that their magnitude affects the ability of a control strategy to converge the vehicle to a desired path. Moreover, they can quantify singularities in the field. An extremum, for example, is marked with curvature $\kappa_S \to \infty$. Therefore, bounding the curvatures guarantees, on one hand, that the vehicle's trajectory stays at a sufficiently large distance from the singularities and, on the other, that the variations of the field are unable to render the control unstable.

Assumption 2: There exist a bound $|\kappa_Q|, |\kappa_S| < \eta$, $\forall \mathbf{r} \in \Omega_S - \Omega_M$.

Building upon these assumptions, an ascending control law should have the goal of transporting the vehicle from any point in Ω_S into Ω_M in finite time. Hence, the problem can be formulated as follows: *given knowledge for the bounds σ and η, design a control law which achieves stable ascending of the trajectory through the potential field S, $\forall\ \mathbf{r}(t) \in \Omega_S - \Omega_M$.*

Theorem 1: Let Assumptions 1 and 2 be satisfied, and let the system (8) evolve under the control law:

$$\omega = K_1 \left(1 - K_2 \frac{dS}{dt}\right), \tag{11}$$

with gains satisfying:

$$K_1 \geq \Theta\sqrt{2}\eta, \tag{12}$$

$$K_2 \geq \frac{1}{\sigma}\left(1 + \frac{\eta}{K_1}\right), \tag{13}$$

where the constant Θ is chosen as $1 < \Theta$ and $\Theta - 1 \ll 1$. Then, given that Ω_S is sufficiently large, there exists a set $\Omega_0, \Omega_M \subseteq \Omega_0 \subseteq \Omega_S$ such that starting from any initial condition in $\mathbf{r}(0) \in \Omega_0$ and $0 \leq \theta(0) \leq 2\pi$, first,

$$\mathbf{r}(t) \in \Omega_S,\ \forall t > 0.$$

and second, there exists time τ, satisfying

$$\mathbf{r}(\tau) \in \Omega_M. \tag{14}$$

Proof: The motion of the vehicle in curvilinear coordinates is given by (10). Note, that $\dot{S} \leq 0$ for $\phi \in [0, \pi]$ and $\dot{S} > 0$ for $\phi \in (\pi, 2\pi)$, therefore the investigation of the system behavior can be reduced to the evolution of the vehicle's orientation relative to the isolines of the potential field. Substituting the control law, (11), into (10) yields

$$\dot{\phi} = K_1 \left(1 + K_2 M \sin\phi\right) - \kappa_S \cos\phi - \kappa_Q \sin\phi.$$

Now, lets assume that $\mathbf{r}(t) \in \Omega_S - \Omega_M$ for $t \in [0, \tau]$, then under K_1,K_2 chosen according to (12), (13), the following inequalities hold.

For $\phi = \pi + \delta$, where δ is a small positive constant, satisfying $\Theta(1 - K_2 M\delta) > 1$, we have

$$\begin{aligned}\dot{\phi} &= K_1 \left(1 - K_2 M \sin\delta\right) + \kappa_S \cos\delta + \kappa_Q \sin\delta \\ &> K_1 \left(1 - K_2 M\delta\right) - \sqrt{2}\eta > 0,\end{aligned} \tag{15}$$

and for $\phi = \frac{3}{2}\pi$, we have:

$$\begin{aligned}\dot{\phi} &= K_1 \left(1 - K_2 M\right) + \kappa_Q < \\ &< K_1 \left(1 - K_2 M\right) + \eta < 0.\end{aligned} \tag{16}$$

Therefore, $\phi \in \left[\pi + \delta, \frac{3}{2}\pi\right]$ is a trapping region for ϕ in which the following holds:

$$0 < \|\nabla S\| \sin\delta < \dot{S}(\mathbf{r}(t)) < \|\nabla S\|. \tag{17}$$

Let t_1 be the time that the orientation enters the trapping region, e.g. $\phi(t_1) \in \left[\pi + \delta, \frac{3}{2}\pi\right]$. Then, the vehicle will ascend the potential field as long as $\mathbf{r}(t) \in \Omega_S - \Omega_M$, which is equivalent to $t_1 \leq t \leq \tau$. Note that,

$$\begin{aligned}\dot{\phi} &\geq K_1 - \kappa_S \cos\phi - \kappa_Q \sin\phi \\ &\geq K_1 - \sqrt{\kappa_S^2 + \kappa_Q^2} > 0,\ \phi \in [0, \pi].\end{aligned} \tag{18}$$

and therefore the vehicle can spend only limited time descending after which its orientation will be confined in the trapping region. Thus, given that Ω_S is sufficiently large, there will exist a set Ω_0, such that if $\mathbf{r}(0) \in \Omega_0$ and $0 \leq \phi(0) \leq 2\pi$ then $\mathbf{r}(t_1) \in \Omega_S$. Moreover, if $\Omega_M \subseteq \Omega_0$ $\mathbf{r}(t) \in \Omega_S$, $\forall t \geq 0$. ■

The implications of this theorem can be better understood if the geometry of the potential field is restricted to a special case - a radial function ($\kappa_Q = 0$). Then, the behavior of the exploration agent can be summarized by the corollary stated below.

Corollary 1: Let $S(\mathbf{r})$ be a radial function , e.g. $S(\mathbf{r}) = S(\|\mathbf{r} - \mathbf{r}_M\|)$, where $\mathbf{r}_M$ are the coordinates of the maximum, and let the control law be:

$$\omega = \eta \left(1 - \frac{1}{\sigma}\frac{dS}{dt}\right). \tag{19}$$

Then

$$\lim_{t \to \infty} \|\mathbf{r}(t) - \mathbf{r}_M\| \to \frac{1}{\eta} \tag{20}$$

$\forall \mathbf{r}(0) \in \Omega_0$ and $\theta \in [0, 2\pi]$.

Proof: The proof proceeds as follows: first, we show that the evolution of the trajectory can be described with a system of two time-invariant differential equations; then, we establish a trapping region for the trajectory; and finally, we prove, that there are no stable limit cycles in the bounded region. In case the last two conditions hold, the Poincare-Bendixson Theorem [13] guarantees that once in the trapping region, the trajectory of the system converges to an equilibrium point within it.

Beginning with the fact that the system evolves in a radial potential field, it follows that there exist an inverse function $S^{-1}(\cdot) = \|\mathbf{r} - \mathbf{r}_M\|$ and that the magnitude of the gradient $\|\nabla S\|$ is also a radial function. Therefore, the system can be expressed in terms of two state space coordinates: the angle ϕ and $\|\mathbf{r} - \mathbf{r}_M\| = -\frac{1}{\kappa_S} = r$ (the minus sign is due to the fact that S is concave). The resulting system yields:

$$\begin{aligned}\dot{r} &= \sin\phi \\ \dot{\phi} &= \eta\left(1 + f\left(r\right)\sin\phi\right) + \frac{1}{r}\cos\phi,\end{aligned} \tag{21}$$

where $f(r) = \frac{\|\nabla S\|}{\sigma}$ and $f(r) > 1$, $\forall r \in \Omega_S - \Omega_M$ (Assumption 1).

Without loss of generality, we will set $\eta = 1$. Equation (20) implies that the trajectory of (21) converges to $r = \frac{1}{\eta} = 1$ and it can be verified that $\{r = 1, \phi = \pi\}$ is a fixed point for the system.

The next step is to establish a trapping region for the trajectory - $\mathcal{T}$, such that if $\{\phi(\tau), r(\tau)\}^T \in \mathcal{T}$, it follows that $\{\phi(t), r(t)\}^T \in \mathcal{T}\ \forall t > \tau$.

By Theorem 1 the trajectory of the vehicle is such that if $\mathbf{r}(0) \in \Omega_0$ then $\mathbf{r}(t) \in \Omega_S, \forall t > 0$, which establishes the first boundary of the trapping region. The other two boundaries are given by $r = 1$, for $\phi \in [\frac{3}{2}\pi, 2\pi]$ and $\phi = \frac{3\pi}{2}$ for $r > 1$. The validity of this boundaries can be directly verified by substituting the corresponding values in (21).

The last side of the trapping region is given by

$$1 - r\cos\phi = 0$$

for $0 \leq \phi < \frac{\pi}{2}$. To verify this boundary, we define the Lyapunov function $L = 1 - r\cos\phi$. Its derivative on the trajectory of the system yields:

$$\dot{L} = r\sin\phi + rf(r)\sin^2\phi. \tag{22}$$

Note, that $\dot{L} > 0$, given that $\mathbf{r} \in \Omega_S$ and $0 \leq \phi < \frac{\pi}{2}$ and therefore the trajectory of the system cannot cross the curve $1 - r\cos\phi = 0$ from within the trapping region.

The boundaries of the trapping region are shown in red in Fig.2.

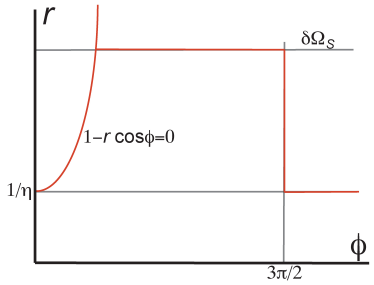

Fig. 2. The boundaries of the trapping region in red for (21)

In the final step of the proof, we use the Dulac Criterion (See Theorem 6.6.3 in [13]) to establish that there are no limit cycles in $\mathcal{T}$. This is done by defining the function $g(\phi, r) = \frac{r^2-1}{\sin\phi}$, which combined with (21) gives:

$$\nabla \cdot (g(\phi, r)\mathbf{F}(\phi, r)) = \frac{(1 - r\cos\phi)(r^2 + 2r\cos\phi + 1)}{r\sin^2\phi}, \tag{23}$$

where $\mathbf{F}$ is the vector consisting of the RHS of (21). It can be verified that $r^2 + 2r\cos\phi + 1 \geq 0\ \forall \phi, r$ and $1 - r\cos\phi \geq 0$ $\forall \phi, r \in \mathcal{T}$, which by the Dulac Criterion implies that there are no stable limit cycles in the trapping region, and therefore the trajectory converges to the fixed point $r = \frac{1}{\eta}$, $\phi = \pi$. ■

The fact that the trajectory converges to a curve with pre-specified radius around the maximum implies that the user can adjust the final distance between the source and the vehicle by adjusting the gain K_1, e.g $K_1 = \frac{1}{r}$. This property can be useful in adversary applications, that require the exploration agent to maintain its existence undetected from the position of the source.

Another property of the control law is that the ascending rate can be adjusted through adjusting the gain K_2. This fact is proved in the next corollary.

Corollary 2: For fixed κ_S, κ_Q and M the growth rate of the potential along the trajectory is a decreasing function of K_2.

Proof: In the prove of Theorem 1, we have established that if K_1 and K_2 are properly assigned, there exist a trapping region for ϕ - $\phi \in (\pi, \frac{3\pi}{2})$. For fixed κ_S, κ_Q and M this translates to a stable fixed point $\phi^* \in (\pi, \frac{3\pi}{2})$ for the one dimensional system given by:

$$\dot{\phi} = K_1\left(1 + K_2 M\sin\phi\right) - \kappa_S\sin\phi - \kappa_Q\cos\phi. \tag{24}$$

It can be verified from this expression that ϕ^* is a decreasing function of K_2 such that as $K_2 \to \infty$, $\phi^* \to \pi$. Taking into account that the descending rate will approach $\dot{S} \to -M\sin\phi^*$, it follows that $\dot{S}$ is also a decreasing function of K_2. ■

What this corollary also implies is that if $S(\mathbf{r})$ is radial function and the magnitude of the gradient, M, is known along the trajectory of the vehicle, a control law of the type (11), having the optimal ascending rate, yields:

$$\omega = K_1\left(1 - \frac{1}{M}\frac{dS}{dt}\right). \tag{25}$$

IV. Applications

In this section, we present two possible applications for the ascending control law.

A. Source centric mapping

The first application of the control is to enable an exploration agent to perform source centric mapping. In this application, the exploration goal is to provide the user with both, a high quality map of the neighborhood of an extremum, and the coordinates of its position. The properties of the ascending/descending control that enable a vehicle to efficiently achieve these objectives are:

1) The ascending/descending algorithm can localize the critical point in the potential field with pre-specified precision.
2) The ascending/descending rate can be adjusted, and along with that the precision with which the vehicle maps the neighborhood of the extremum.

The first property can be traced back to Theorem 1 where we have shown that for any size of the set Ω_M, as long as Assumptions 1 and 2 are satisfied, there exist gains K_1 and K_2 that can converge the vehicle's trajectory to Ω_M.

The second one can be drawn as a direct consequence of Corollary 2. In addition, it will also amount to the trajectory of the vehicle spending less time in areas where the magnitude of the gradient is small, as opposed to areas where the magnitude of the gradient is large. This property is visualized in Fig. 3 where the vehicle is ascending a radial potential field given by:

$$S(\mathbf{r}) = -\|\mathbf{r}\| + 5\sin\left(\frac{\|\mathbf{r}\|}{7}\right). \tag{26}$$

This figure clearly shows that the trajectory is concentrated in the lighter regions, corresponding to large $\|\nabla S\|$, as opposed to the darker regions, corresponding to small $\|\nabla S\|$.

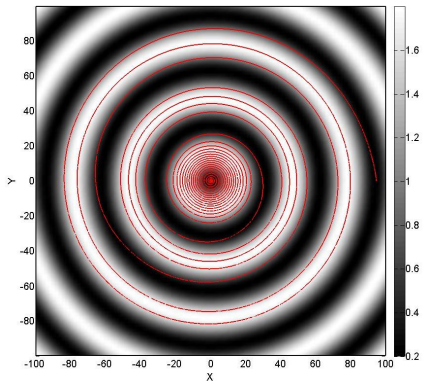

Fig. 3. The trajectory of the vehicle for $K_1 = 5$, $K_2 = 40$ and $S(\mathbf{r})$ given by (26), shown over a map of $\|\nabla S\|$

In Fig. 4, we show the control law applied to a more realistic situation. The potential field pictured represents the total CO_2 concentration near the surface of the Pacific Ocean, off the coast of South America [14]. In the left image, one can observe the trajectory of the vehicle along the potential field, and in the right image, the map reconstructed from the gathered data.

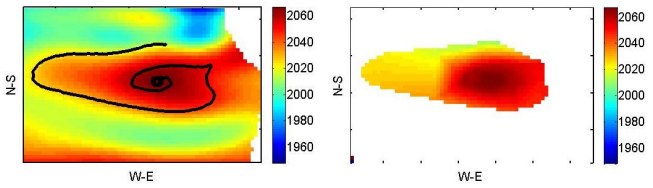

Fig. 4. The trajectory of the vehicle for $K_1 = 1$, $K_2 = 2.5$ in the potential field pictured above and the reconstructed map of the potential field from the data gathered along the trajectory of the vehicle

B. Source-tracking

We are assuming that the source (further referred as the target) moves in the plane and emits a potential, which is a constant function of the distance between the target and the pursuing vehicle.

To accommodate for the moving target, the model described in (10) should be appended. Defining γ to be the angle between the tangent to the isoline at the position of the tracker and the heading of the target, the following new system describes the evolution of the potential at the position of the pursuer:

$$\begin{aligned} \dot{S} &= M\left(-\sin\phi + V_t \sin\gamma\right) \\ \dot{\phi} &= \omega - \frac{1}{r}\left(-\cos\phi + V_t\cos\gamma\right) \\ \dot{\gamma} &= \omega_t - \frac{1}{r}\left(-\cos\phi + V_t\cos\gamma\right). \end{aligned} \tag{27}$$

The parameters V_t and ω_t are respectively the velocity and the steering rate of the target, and r is the distance between the target and the pursuer.

Building upon Theorem 1, it should be possible to compensate for the new terms by modifying the gains K_1 and K_2. Before following this proposition, however, we restrict the mobility of the target with the following new assumption:

Assumption 3: The target moves with constant velocity $V_t < V_{max} < 1$ and $\omega_t = 0$.

This assumption will be alleviated in future work to accommodate for linear acceleration and steering velocities. Further in this section, we show simulation results for tracking a target maneuvering with constant steering rate ω_t.

Proposition 1: If Assumptions 1, 2 and 3 are satisfied, there exist a control law of the type:

$$\omega = K_1\Theta_1\left(1 - K_2\Theta_2\frac{dS}{dt}\right), \tag{28}$$

for which if the pursuing vehicle is in the proximity of the target it will reach Ω_M in finite time, where K_1 and K_2 are given by Theorem 1 and Θ_1, $\Theta_2 > 1$.

Proof: Proving this proposition is equivalent with proving that the distance between the target and the pursuer will be decreasing, or, in other words, the potential measured at the position of the pursuer will be increasing. This yields to the condition:

$$\dot{S} > M\epsilon > \sigma\epsilon > 0, \tag{29}$$

where ϵ is a small positive constant and σ is defined in Assumption 1.

Further, lets assume that there exist a trapping region $\mathcal{T}$ in the $\{\phi, \gamma\}$ plane such that if $\{\phi(\tau), \gamma(\tau)\} \in \mathcal{T}$, it follows that $\{\phi(t), \gamma(t)\} \in \mathcal{T}$, $\forall t > \tau$. Then, the proof transforms to proving that there exist ϵ such that:

$$\inf_{\{\phi,\gamma\}\in\mathcal{T}}\left(-\sin\phi + V_t\sin\gamma\right) > \epsilon, \tag{30}$$

given that the parameters in (27) obey Assumptions 1 through 3.

We start with the set $\mathcal{T} = \{\phi \le \frac{3}{2}\pi | -\sin\phi + V_t\sin\gamma \ge \epsilon\}$, where ϵ is chosen such that:

$$(1 - V_{max}) > 2\epsilon. \tag{31}$$

Note that the so defined $\mathcal{T}$ satisfies (30). To prove that it is also a trapping region, $\phi = \frac{3}{2}\pi$ is substituted into the second equation of (27), which yields:

$$\dot{\phi} = K_1\Theta_1\left(1 - K_2 M\Theta_2\left(1 + V_t\sin\gamma\right)\right) - \frac{1}{r}V_t\cos\gamma.$$

The gain K_1 is given by (12). Therefore, choosing Θ_2 as $\Theta_2 > \frac{\Theta_1 + V_{max}}{\Theta_1(1 - V_{max})}$ guarantees that $\dot{\phi} \le 0$ and hence, establishes $\phi \le \frac{3}{2}\pi$ as a valid bound for the trapping region.

On the other hand, defining the Lyapunov function:

$$L = -\sin\phi + V_t\sin\gamma - \epsilon, \tag{32}$$

and proving $\dot{L} > 0$ for $L = 0$, $\phi \in (\pi, \frac{3}{2}\pi)$ establishes the other bound for the trapping region. Differentiating on the trajectory yields:

$$\dot{L} = -\omega\cos\phi - \frac{1}{r}\left(-\cos\phi + V_t\cos\gamma\right)^2, \tag{33}$$

where ω is given by (28).

Note that $\dot{L} \ge 0$ should be satisfied on the curve $L = 0$, when ϕ is in $(\pi, \frac{3}{2}\pi)$. This fact can be utilized in the following expression for $\cos\phi$:

$$\cos\phi = -\sqrt{1 - (V_t\sin\gamma - \epsilon)^2}. \tag{34}$$

Therefore, the condition $\dot{L} \geq 0$ for $L = 0$ transforms to:

$$\omega_\epsilon \geq \frac{1}{r} \frac{\left(\sqrt{1-(V_t \sin\gamma - \epsilon)^2} + V_t \cos\gamma\right)^2}{\sqrt{1-(V_t \sin\gamma - \epsilon)^2}}, \quad (35)$$

where ω_ϵ is derived from setting $L = 0$ in (28):

$$\omega_\epsilon = K_1\Theta_1 \left(1 - K_2\Theta_2\epsilon\right). \quad (36)$$

Letting $\epsilon \to 0$ transform the condition expressed in (35) into:

$$K_1\Theta_1 \quad \geq \quad \frac{1}{r}(1+V_t)^2, \quad (37)$$

where we have used that:

$$\frac{\left(\sqrt{1-(V_t \sin\gamma)^2} + V_t \cos\gamma\right)^2}{\sqrt{1-(V_t \sin\gamma)^2}} \leq (1+V_t)^2 \quad (38)$$

Taking into account that both the left and the right side of (35) are continuos function of ϵ, if we choose $\Theta_1 > (1 + V_{max})^2\Theta$, where $1 < \Theta$ and $\Theta - 1 \ll 1$, there will exist $\epsilon > 0$ for which (35) is satisfied. Then, the trapping region is defined by both curves - $-\sin\phi + V_t \sin\gamma - \epsilon = 0$ and $\phi = \frac{3}{2}\pi$, and its existence is guaranteed by setting:

$$\Theta_1 \quad \geq \quad \Theta(1+V_{max})^2 \quad (39)$$

$$\Theta_2 \quad \geq \quad \frac{\Theta_1 + V_{max}}{\Theta_1\left(1 - V_{max}\right)}. \quad (40)$$

■

In Fig. 5, we show the trajectories of both the pursuer and the target for a potential function given by $S(\|\mathbf{r}\|) = \|\mathbf{r}\|$, which is equivalent of assuming that the intensity function is known. In Fig. 6, we show $\|\mathbf{r}\|$ as function of time during the pursuit.

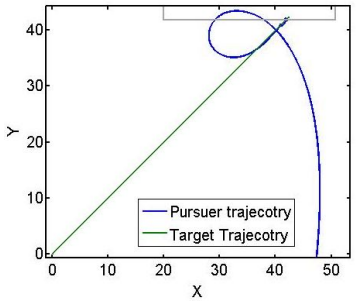

Fig. 5. The vehicle pursuing a target - $K_1\Theta_1 = 2.25$, $K_2\Theta_2 = 2$

In Fig. 7, we show a pursuit for which $\omega_t = 0.1$.

V. Concluding remarks

In this paper, it has been shown that a sensor enabled robot can be controlled to approach maxima (or minima) of a sensed potential field. The conditions under which our proposed control law can be guaranteed to work are regularity assumptions regarding the field. The results of the paper, combined with our previous work, provide a set of motion primitives for exploration of a potential field by a single robotic agent. Future work will emphasize such exploration using teams of robots.

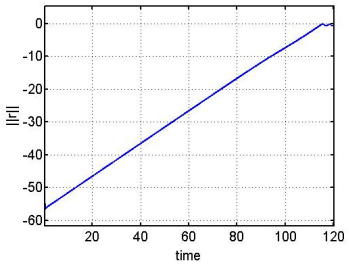

Fig. 6. The distance between the pursuer and the target as a function of time

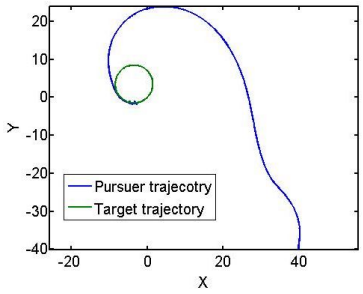

Fig. 7. The vehicle pursuing a target in case of $\omega_t = 0.1$ and $K_1\Theta_1 = 2.25$, $K_2\Theta_2 = 2$

References

[1] D. Baronov and J. Baillieul, "Reactvie exploration through following isolines in a potential field," in *Proceedings of the American Control Conference*, 2007, pp. 2141–2146.

[2] N. E. Leonard, D. Paley, and F. Lekien, "Collective motion, sensor networks and ocean sampling," *Proceedings of the IEEE*, 2006.

[3] P. Orgen, E. Fiorelli, and N. E. Leonard, "Cooperative control of mobile sensor networks: Adaptive gradient climbing in a distributed environment," *IEEE TRANSACTIONS ON AUTOMATIC CONTROL*, vol. 49, no. 8, pp. 1292–1302, August 2004.

[4] A. Lilienthal and T. Duckett, "Creating gas concentration gridmaps with a mobile robot," in *Intelligent Robots and Systems (IROS)*, vol. 1, 2003, pp. 118–123.

[5] A. Hayes, A. Martinoli, and R. M. Goodman, "Distributed odor source localization," *Sensors Journal, IEEE*, vol. 2, no. 3, pp. 260–271, June 2002.

[6] F. Zhang and N. E. Leonard, "Generating contour plots using multiple sensor platforms," *IEEE Swarm Intelligence Symposium*, 2005.

[7] S. Susca, S. Martinez, and F. Bullo, "Monitoring environmental boundaries with a robotic sensor network," *ACC*, 2006.

[8] A. Ganguli, S. Susca, S. Martinez, F. Bullo, and J. Cortes, "On collective motion in sensor networks:sample problems and distributed algorithms," in *Proceedings of the 44th IEEE Conference on Decision and Control, and the European Control Conference*, 2005.

[9] C. G. Mayhew, R. G. Sanfelice, and A. R. Teel, "Robust source-seeking hybrid controllers for autonomous vehicles," in *2007 American Control Conference, Marriott Marquis Hotel at Times Square, New York City, USA*, 2007.

[10] S. B. Andersson and D. Y. Abramovitch, "A survey of non-raster scan methods with application to atomic force microscopy," in *Proceedings of the American Controls Conference*, July 2007.

[11] J. Baillieul and L. McCoy, "The combinatorial graph theory of structured formations," in *Proceedings of the 46-th IEEE Conference on Decision and Control*, New Orleans, December 2007.

[12] D. Baronov, S. B. Andersson, and J. Bailliuel, "Tracking a nanosize magnetic particle using a magnetic force microscope," in *to appear in Proceedings of the 46-th IEEE Conference on Decision and Control*, New Orleans, December 2007.

[13] R. C. Robinson, *An Introduction to Dynamical Systems: Continuous and Discrete*. Pearson Prentice Hall, 2004, pp. 208–209.

[14] {Carbon Dioxide Information Analysys Center, Environment Sciences Division, Oak Ridge National Laboratory}. [Online]. Available: http://cdiac3.ornl.gov/